

# Accepted Manuscript

Aggregation propensity of amyloidogenic and elastomeric dipeptides constituents†

Vikas Kumar, K. Vijaya Krishna, Shruti Khanna, Khashti Ballabh Joshi



PII: S0040-4020(16)30645-7

DOI: [10.1016/j.tet.2016.07.022](https://doi.org/10.1016/j.tet.2016.07.022)

Reference: TET 27918

To appear in: *Tetrahedron*

Received Date: 3 May 2016

Revised Date: 21 June 2016

Accepted Date: 6 July 2016

Please cite this article as: Kumar V, Krishna KV, Khanna S, Joshi KB, Aggregation propensity of amyloidogenic and elastomeric dipeptides constituents†, *Tetrahedron* (2016), doi: 10.1016/j.tet.2016.07.022.

This is a PDF file of an unedited manuscript that has been accepted for publication. As a service to our customers we are providing this early version of the manuscript. The manuscript will undergo copyediting, typesetting, and review of the resulting proof before it is published in its final form. Please note that during the production process errors may be discovered which could affect the content, and all legal disclaimers that apply to the journal pertain.

## Graphical Abstract

To create your abstract, type over the instructions in the template box below.  
Fonts or abstract dimensions should not be changed or altered.

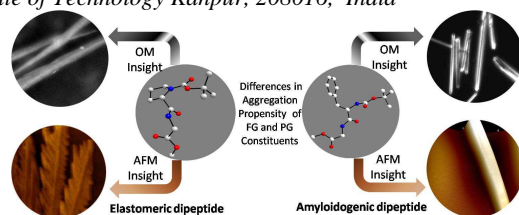
### Aggregation Propensity of Amyloidogenic and Elastomeric Dipeptides Constituents<sup>†</sup>

Leave this area blank for abstract info.

Vikas Kumar<sup>a</sup>, K. Vijaya Krishna<sup>b</sup>, Shruti Khanna<sup>b</sup>, and Khashti Ballabh Joshi<sup>\*a</sup>

<sup>a,\*</sup> Department of Chemistry, School of Chemical Science and Technology, Dr Harisingh Gour Central University Sagar, MP, 470003, India. E-mail: [kbjoshi77@gmail.com](mailto:kbjoshi77@gmail.com); [kbjoshi@dhsu.ac.in](mailto:kbjoshi@dhsu.ac.in),

<sup>b</sup>Department of Chemistry, Indian Institute of Technology Kanpur, 208016, India





# Aggregation Propensity of Amyloidogenic and Elastomeric Dipeptides Constituents<sup>†</sup>

Vikas Kumar<sup>a</sup>, K. Vijaya Krishna<sup>b</sup>, Shruti Khanna<sup>b</sup> and Khashti Ballabh Joshi<sup>\*,a</sup>

<sup>a,\*</sup> Department of Chemistry, School of Chemical Science and Technology, Dr Harisingh Gour Central University, Sagar, MP, 470003, India.

E-mail: kbjoshi77@gmail.com; kbjoshi@dhgsu.ac.in.

<sup>b</sup> Department of Chemistry, Indian Institute of Technology Kanpur, 208016, India

## ARTICLE INFO

### Article history:

Received

Received in revised form

Accepted

Available online

## ABSTRACT

This study demonstrates the self-assembly of N- and C-terminal protected dipeptides Phe-Gly and Pro-Gly which were derived from amyloidogenic and elastomeric peptide sequences. These constituents afforded nanostructured supramolecular ensembles through various non-covalent interactions in the solid state which can be directly correlated with their fibrillation event in solution phase. Interestingly microscopic observations revealed that the amyloidogenic dipeptide constituents assembled into hollow tubular structures whereas the elastomeric dipeptide constituents assembled into the feather or sheet like structures.

**Keywords:** Peptide, Self assembly, Fibrillation, Amyloidogenic, Elastomeric

2009 Elsevier Ltd. All rights reserved.

## Introduction

The fundamental topological property of proteins and polypeptides is the formation of three dimensional architectures that are used to the greatest advantage by nature for molecular recognition<sup>1-6</sup> and its functions in biological systems. To understand the primary principles which direct the architecture of such motifs is a necessity for probing the origin of many physical, biophysical, and biomedical phenomena related to specific diseases.<sup>7,8</sup> The common supramolecular motifs, helical and sheet like arrangements are found in all functional proteins. The challenging area of research in the ground of ordered supramolecular peptide assemblies by means of short peptides has been much focused in recent years.<sup>9,10</sup>

In this context, proteins and polypeptides, which are molecular determinants of elasticity, are highly demanded. Elastomeric proteins are well known for their robustness and elasticity and are present in a wide range of living organisms.<sup>11-17</sup> Disorderliness in their structures and associated hydration are important features of the elastomeric proteins.<sup>18-21</sup> Nucleoporins,<sup>22-26</sup> Tropoelastin,<sup>27,28</sup> Spider Silk<sup>29-35</sup> and Resilin<sup>36-39</sup> are few examples of natural disordered proteins with elastomeric function. These elastomeric proteins are rich in amino acid sequences mainly; Phenylalanine (F), Proline (P) and Glycine (G), however they all are widely varying in their amino-acid content along with the dipeptide Phe-Gly and Pro-Gly repeat.<sup>40-42</sup> For example Nucleoporins; which are the constituent building blocks of,

the nuclear pore complex (NPC) forming the gateway to regulate the flow of macromolecules between the cell nucleus and the cytoplasm contain FG peptide repeats which forms major components of NPC.<sup>43-52</sup> Large number of protein molecules can be transported by a single NPC every minute. About 50 repeat units of FG making clusters of hydrophobic groups become unfolded during the passage of protein and RNA through NPC and get converted into three dimensional cluttered structures with hydrogel-like properties. Various approaches have applied to explore the nature of FG domain and it is found that flexible brush like unfolded structures exist and exhibit entropic elasticity.

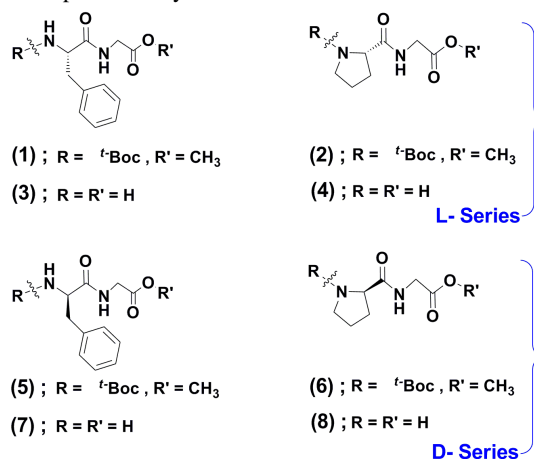


**Figure 1.** Molecular structure of protected and deprotected dipeptides, *Top*: dipeptides with L-amino acid, and *Bottom*: with D-amino acid.

Apart from FG, PG also often appears in the sequence of disordered proteins like spider silk. Both Proline and Glycine contribute to disorder the protein but differently.<sup>53-64</sup> Proline which contain cyclic five membered side chain and known for its rigid structure, is stiff and highly restricted, disturbing the secondary structure formation of protein. Whereas Glycine, is known for its flexibility and lacking any side chain whose order is entropically unfavourable. However the composition of Proline and Glycine affect their amyloid formation tendency and elasticity.<sup>65-67</sup> For example the elastic nature of silk fiber was shown to correlate with high glycine content by measurements from circular dichroism spectroscopy. The main constituent of amyloidogenic peptide A $\beta$ 42 is Phe-Phe recognition motif and by replacing the one constituent of this motif with other non aromatic amino acid showed lower aggregation propensity compare to higher-order self assembled structures of Phe-Phe.<sup>68</sup> Amyloid fibrils are associated with tissue degenerative diseases whereas elastin provides extensible tissues including skin and arteries. Though self organization of these proteins into fibrils is common phenomenon associated with both the systems but the physical properties and energy contribution for other biomedical applications of these systems are poorly resolved.

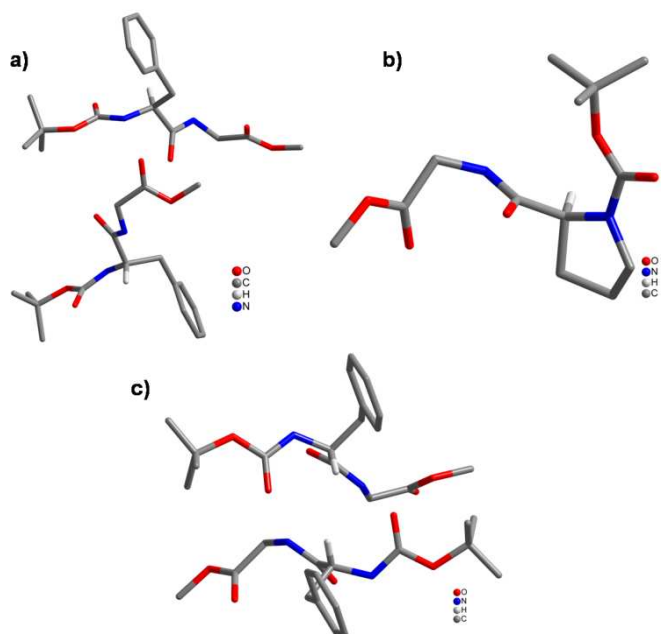


**Figure 2.** Solid state structure of (a) **1**, (b) **2** and (c) **5** (hydrogen atoms are omitted for the sake of clarity). Color code; blue, nitrogen; red, oxygen; gray, carbon.

## Results and Discussions

Based on the above literature information, it is possible that elastomeric and amyloidogenic peptides can be differentiated by applying simple chemical and physical changes in shortest peptides *viz* dipeptides. In order to understand the fundamental behaviour of the self assembly of amyloid or elastin like protein aggregates, we designed a set of D and L- dipeptides sequences constituted by FG and PG having physico-chemical properties compatible with those of the hydrophobic domains of amyloid fibrils, as well as elastin respectively. Since our growing interest in peptide self assembly and its application in biomedical field,<sup>69-72</sup> encouraged us to study widely the assembling behaviour of all the protected and deprotected dipeptides. Therefore we have strategically designed (Fig. 1) the two model dipeptides; where the second amino acid, i.e. glycine residue was intact in both peptides but the alteration in the first amino acid *viz* phenylalanine and proline. To understand the fundamental mechanism of these peptides in relation to self assembly we wish

to see the nature of non-covalent interactions, both in solution and solid state<sup>73-75</sup> and to understand how subtle change of a dipeptide sequence can alter the self-assembly and the nano-structure formation.

We started this work by correlating the solid state structure of protected dipeptides with solution-phase aggregation. Crystals of protected dipeptides **1**, **2** and **5** suitable for X-ray diffraction studies, were grown by careful, time dependent slow evaporation of solvent methanol/cyclohexane (~70:30). However our several attempts fail to grow the crystals of conjugate **6** and deprotected D and L dipeptides.<sup>76</sup> It was found that all three protected dipeptides crystallize in orthorhombic space group P21 21 21 (No. 19) (Fig. 2). Crystallographic signature of **1**, **2** and **5** displayed the difference in solid state conformation,<sup>77-80</sup> which perhaps is the basis of significant difference in ordered self-assembly. A tabulated comparison of torsional angles of **1** (as representative for **5** also) and **2** reveal that the difference in solid state conformation. Most of the torsional angles,  $\phi_1$ ,  $\psi_1$ ,  $\phi_2$  and  $\psi_2$  values of the constituent amino acids residues for the compound **1** fall within the polyproline II (PP-II) structural<sup>77</sup> region, however for compound **2** the torsional angles  $\phi_1$ ,  $\psi_1$ ,  $\phi_2$  and  $\psi_2$  values (table 1) of the constituent amino acids residues fall only in the Collagen fiber region of the Ramachandran plot.<sup>81</sup>

**Table -1** Selected torsional angles of compound **1** and **2**.

L-Boc-Phe-Gly-OMe		L-Boc-Pro-Gly-OMe	
Torsion Angles	Value	Torsion Angles	Value
$\omega_1$	171.2 (2)	$\omega_1$	-12.8 (4)
$\phi_1$	-88.9 (3)	$\phi_1$	-51.6 (4)
$\psi_1$	163.7(2)	$\psi_1$	142.8 (3)
$\omega_2$	176.2 (3)	$\omega_2$	170.5 (3)
$\phi_2$	-122.1(3)	$\phi_2$	-64.4 (4)
$\psi_2$	-15.6 (4)	$\psi_2$	154.8 (3)

A time-dependent aggregative propensity of **1** and **2** was evaluated by dark field optical microscopic imaging at 63X magnification. Fresh solution of **1** (3 mM) in 50% methanol-water, did not reveal any significant and noticeable self-assembly under optical microscope, but long straight tubular fibers were evident after 2 days of incubation at ambient temperature (Fig. 3a). A continued

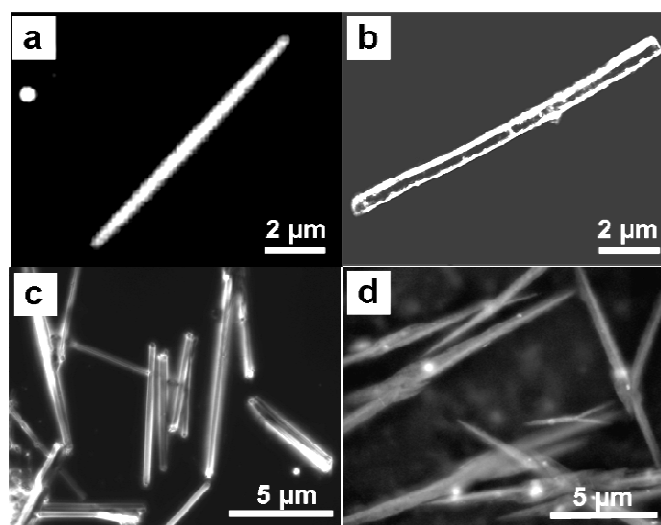


**Figure 3.** Optical micrographs of self-assembled morphology by **1**, (a) after 36 h, (b) 42 h, (c) 48 h, incubation (d) Optical micrographs of self-assembled morphology of fresh sample of **2** in dark field condition.

follow up confirmed that 42 hours incubation time period changed the dimensions of tubular structures. The diameter of these tubular

structures increases from 0.6 micron to 1.0 micron and length increased from 1 micron to several micrometers. The lumen of tubular fiber visualized, hints hollowness of these tubular fiber from inside. However, no solvent molecules have been crystallographically detected inside the cavity. Amorphous aggregates and well developed straight hollow tubular fibers were observed on incubation of **1** up to 48 hours at ambient temperature (Fig. 3c). However the protected compound **2** showed long straight fibers at fresh condition only (Fig. 3d).

To understand the nature of time dependent self assembly, 1 mM solution of conjugate **1**, as representative molecule, and 10  $\mu$ M fluorescein solutions were co-incubated at ambient temperature, in 50% methanol/water solvent. This stock solution was equally divided into six portions and transferred into six separate eppendorf tubes. A 20  $\mu$ L aliquot of fresh and the aged solution of different time interval *viz* 0, 8, 16, 24, 32 and 40 h from the different respective tubes were loaded on a glass slide and dried at room temperature followed by imaging under a fluorescence optical microscope.

Interestingly, instantaneous formation and appearance of spherical structures were observed at time 0 h which were organized into a compact colony of spherical structures from time 8 h to 32 h and finally transformed into fibrillar/tubular structures after 40 h of incubation (Fig. 4). This time dependent study reveals that formations of tubular structures are thermodynamically stable. When considering the transformation of spherical aggregates to defined tubular structures, thermodynamic factors should also be invoked.

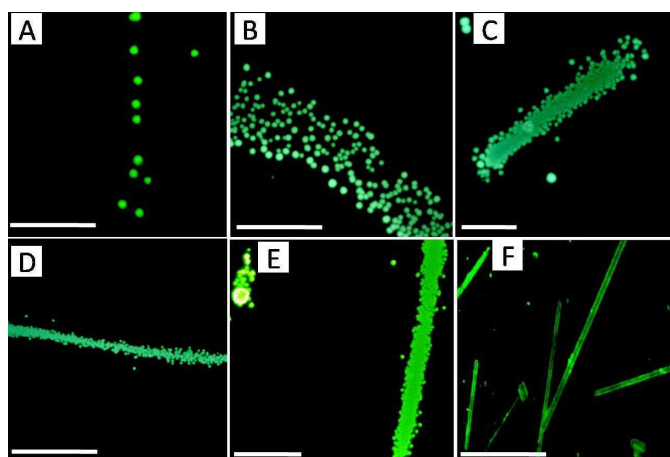


**Figure 4.** Fluorescence optical micrographs of conversion of spherical aggregates of **1** into tubular structures; at (A) 0 h, (B) 8 h, (C) 16 h, (D) 24 h, (E) 32 h and (F) 40 h incubation. Scale bar 20  $\mu$ m

The typical condition for the formation of crystals of conjugate **1**, **2** and **5** are time dependent slow evaporation at ambient temperature and the identical applied conditions also accelerate the transformation of spherical aggregates into tubular structures observed under optical microscope.<sup>82-84</sup> It has been noted that the prolonged incubation at ambient temperature promoted the ordering of random aggregates into ordered one and therefore commensurate with energetic factors which supported the growth of random aggregates in a particular directions.

Further to check the self assembly process of D-isomer, **5**, which was only differing in its chirality, we prepared a fresh solution of **5** and imaged under AFM. The freshly prepared solution of **5** revealed uniformly distributed punctuated structures over the mica surface (Fig. 5A), while incubating it for 12 h the solution of **5** resulted prefibrillar aggregates (Fig. 5B) confirming a time dependent fibrillation event too. At 36 h of incubation these aggregates get partially converted into fibrillar/tubular structures, where the association of spherical aggregates clearly visualized, which is further confirmed by its 3D image (Fig. 5C, D). The prolonged incubation of this solution leads to the formation of robust

rod like assembly (Fig. 5E, F).<sup>85-89</sup> The AFM observations are well corresponded with OM data of figure 4 and further confirmed that both D- and L- isomers perhaps followed the same energetic during the formation of tubular structures.

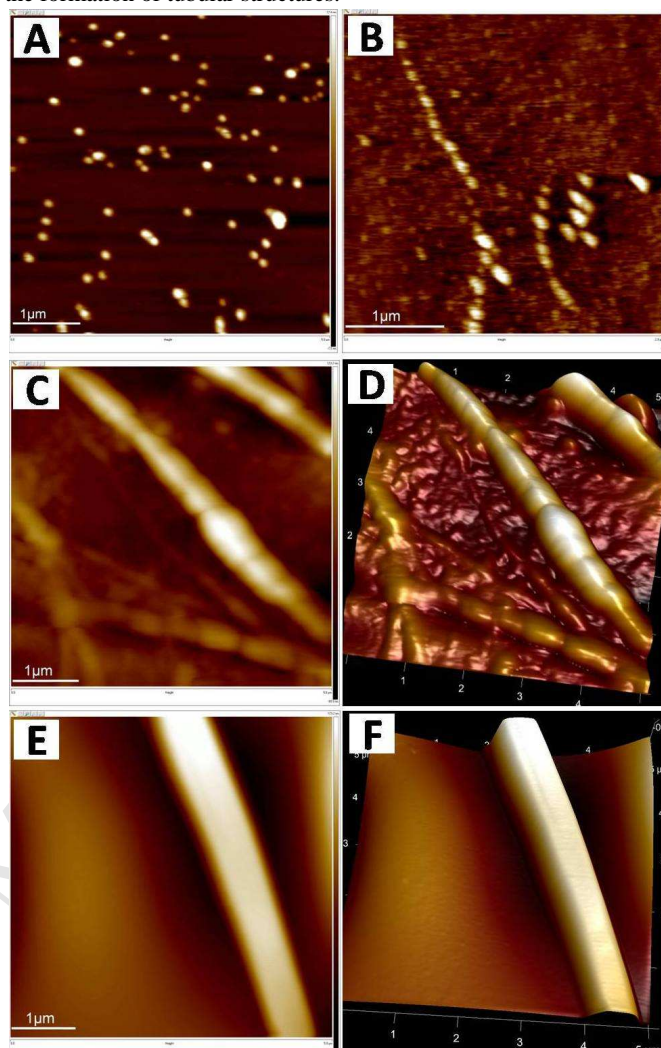


**Figure 5.** AFM micrographs of conversion of spherical aggregates of **5** into rod like structures; at (A) 0 h, (B) 12 h, (C) 36 h, and (D) 48 h incubation, (E) formation of robust rod like assembly and (F) corresponding 3D structure.

To check the self assembly of all the protected dipeptide conjugate, we have used 3 days incubated samples of **1**, **2**, **5** and **6**. The solutions of these samples were spread over the surfaces of freshly cleaved mica followed by AFM imaging. The image analysis revealed that protected dipeptide constituted by D and L isomers of phenylalanine i.e. **1** (Fig. 6A) and **5** (Fig. 5, 6C) are forming similar robust structures which are almost similar in morphology whereas the compound **2** giving robust feather or sheet like structures which are composed of small fibers and **6** (Fig. 6D) assembled into flexible thin fibers as compared to **2** (Fig. 6B). Therefore we did not observe any major morphological change in the self assembly of **1** and **5** however, our observations reveal that protected dipeptide **2** and **6** show little variation in their self assembly process, which could perhaps be due to the amorphous nature of **6** as compared to **2** and hence did not get crystallize.

We further investigated the time dependent self assembly process of the deprotected analogues of these protected compounds i.e. **3**, **4**, **7** and **8** (Fig.7). The freshly prepared 1 mM solution of all these deprotected compounds in 50% methanol-water self assembled into defined morphology. The compound **3** shows flexible fiber formation while **7** assembled into straight rod like morphology. In contrast to

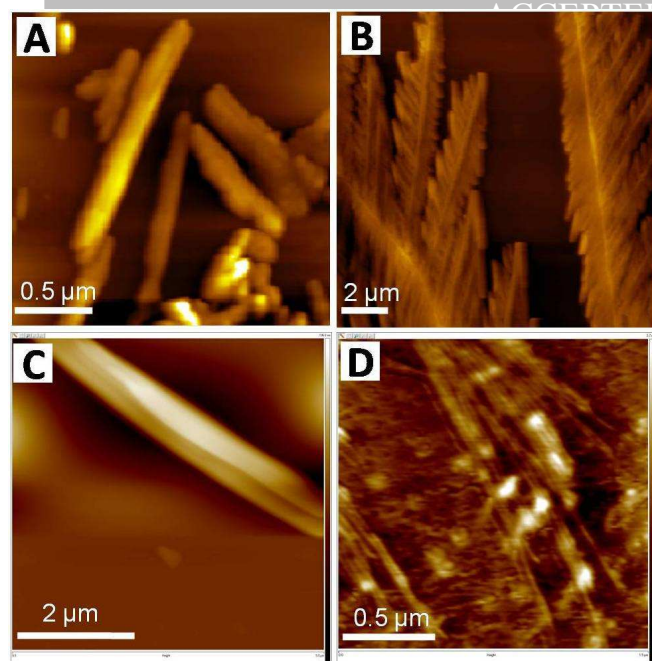


**Figure 6.** AFM micrographs of 3 days aged samples of L and D conjugates of **1**, **2**, **5** and **6**. (A) 3 days aged sample of **1** showing tubular structures, (B) sample of **2** showing sheet like structures, (C) sample of **5** also showing robust tubular like structures and (D) sample of **6** showing long thin fibers.

this fresh sample of proline containing compounds **4** and **8** rapidly assembled into extensive thin fibers perhaps due to the increase in non-covalent interaction compare to protected one and hence can work as gelants upon changing solvents. Such type of different behavior in self-assembling morphology among these compounds is due to the presence of hydrophobic groups such as *t*-Boc and OMe and variation of two amino acids specifically phenylalanine an

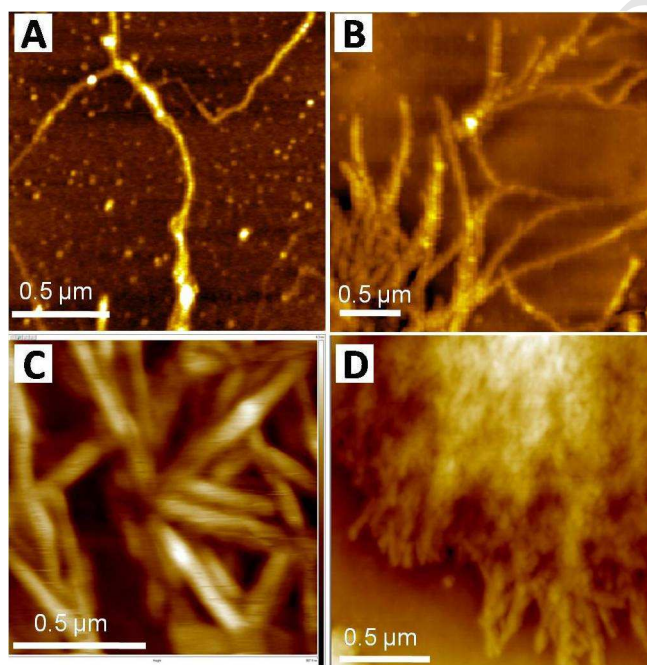


**Figure 7.** AFM micrographs of fresh samples of deprotected L and D conjugates **3**, **4**, **7** and **8**. Figure depicts: (A) thin flexible fibrillar structures of **3**, (B) formation of extensive branch like structures from **4**, (C) robust tubular like structures of **7** and (D) extensive fibrillation event in **8**.

aromatic side chain substituent and proline which is also known for its structure breaking role and rigidity in various peptides<sup>77</sup> and

protein. All compounds have one flexible amino acid glycine which is covalently linked with the phenylalanine and proline, and known for its trivial hydrophilicity which may increase the solution state intermolecular or intramolecular hydrogen bonding. If the N and C-terminus of these peptides are free the non-covalent interactions will get enhanced hence assembled rapidly. In case of the dipeptides which contain Phe residues will show slightly different behavior due to the intervention of aromatic side chain in the mixture of polar organic and inorganic solvents (50% aqueous methanol). Therefore AFM microscopic investigations of protected and deprotected dipeptides reveal that aggregation propensity of all these conjugates behave differently. Further to understand the nature of the fibrous morphology obtained by AFM we have recorded the PXRD of fibers and compared with X-Ray pattern from crystallography. The solution of peptides samples deposited over the glass surface followed by drying produced thin film of thick fibers. The observations from PXRD pattern reveal that mostly all the fibers are amorphous in nature (data not shown).

Therefore at this stage to understand the solution state self-assembly process of these conjugates and its correlation with solid state structures and assembly, we have taken **1** and **2** as representative molecules (Fig. 8). We did the <sup>1</sup>H NMR titration in various ratios of CH<sub>3</sub>OH in CDCl<sub>3</sub> (0-40%) to explain the effect of possible non covalent interactions via the respective participation of amido -NH, aromatic, Phe- $\alpha$  and Pro- $\alpha$  key protons in the self-assembly process.<sup>90, 91</sup> The downfield chemical shifts of the amide protons of **1** and **2** and upfield chemical shifts of aromatic, Phe- $\alpha$  and Pro- $\alpha$  of compound **1** and **2** proton(s) respectively was evident through an incremental addition of CH<sub>3</sub>OH in CDCl<sub>3</sub>. A marked movement of key proton resonances is suggestive of the crucial role of intermolecular  $\pi$  stacking and hydrogen bonding interactions in the supramolecular ensemble of **1** and **2** in solution state (Fig. 8).

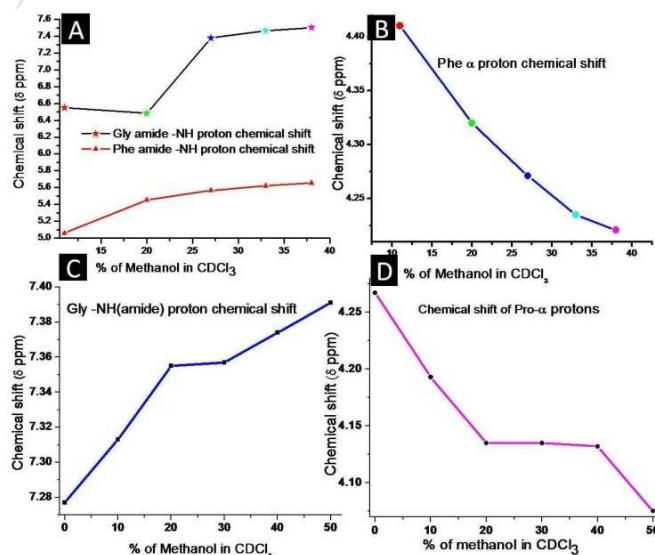


**Figure 8.** <sup>1</sup>H NMR titration experiments of representative compound **1** (top) and **2** (bottom) in the presence of increasing amount of CH<sub>3</sub>OH. The titration experiments were performed in the CDCl<sub>3</sub> solvents. The remarkable change in the key protons were observed and correlated with solid state structures.

Further these noncovalent and other short contacts were clearly visualized in the solid state structures of these molecules and supported by literature too. For example the ...C-H... $\pi$  interaction was found in the solid state structure of **1** where the ...C-H of *t*-Boc group was directly showing the interaction with aromatic ring of another molecule in the same unit cell. We have further investigated this behavior with the help of <sup>1</sup>H NMR titration experiment where

upon incremental addition of the polar solvent, CH<sub>3</sub>OH, showed up field shift for <sup>1</sup>H Boc protons and aromatic protons (Fig. 9). The solid state structure (Fig. 2b) of the compound **2** also supports these observations in which the inter and intramolecular hydrogen bonding distances range from 2.07 Å – 2.84 Å and other short contacts which are from 2.36 Å- 3.33 Å stabilizes the crystal packing. These factors are perhaps responsible for the rapid self-assembly of **2** (Fig. 6B) and it's deprotected conjugate **8** in solution state too. These observations reveal that upon simple side chain modification one can transform the nature of self-assembly which will be useful for several nanotechnological applications.

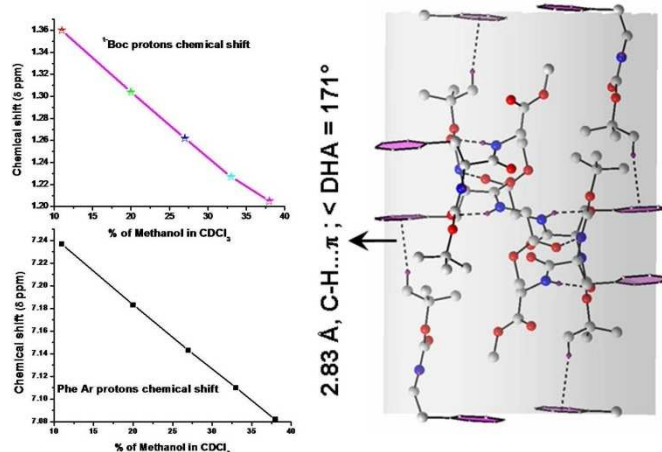


**Figure 9.** <sup>1</sup>H NMR titration experiments of compound **1** in the presence of increasing amount of CH<sub>3</sub>OH. The figure depicts that the remarkable downfield shift in <sup>1</sup>H Boc and Phe aromatic protons noted and correlated well with solid state structure of **1**.

Other than circular dichroism (CD) spectroscopy, FTIR spectroscopy has also been used to evaluate protein secondary structure. The specific and qualitative information can also be obtained by using FTIR spectroscopy, a larger group of peptides and protein features can be classified especially relating specific Amide I and Amide II bands to secondary structure. By comparing the intensity ratios of these two bands we can easily determine the amount of secondary structures before and after the incubation of peptides.<sup>99-101</sup> Therefore we recorded the FTIR spectra of two representative compounds to access information about the secondary structures in self-assembled peptide nanostructures described here. We have now taken the FTIR of fresh and incubated (fibers) samples. Interestingly the observations from FTIR reveal that there is change in secondary structures after the incubation of samples. We have taken the solution of fresh samples of protected FG and PG peptides in appropriate amount as a representative molecules followed by lyophilization. When the solvent was removed completely the samples were ready for IR measurement. The FTIR spectra showing the differences in main functional group absorbances when compared with FTIR spectra of corresponding fresh samples. The changes in the Amide I, Amide II, aromatic and aliphatic regions of these peptides giving hint that there is a significant change in the secondary structures (ESI) which is well corresponded with AFM micrographs where we observed the formation of well defined aggregates or fibers.<sup>102</sup>

Based on all the above information, we decided to construct a structural model to understand the emergence of distinct morphological structures by changing side chain substituent's in simple dipeptides. Therefore we have taken **1** as representative molecule. Model figure depicts (Fig. 10) that in solid state the molecules of **1** arranged in a columnar fashion when viewed along "a" axis (Fig. 10). The elongation of crystal packing which is mainly stabilized by hydrogen bonding and displaced  $\pi$ - $\pi$  stacking<sup>92</sup> and showed the distance between two aromatic rings i.e. 5.39 Å along

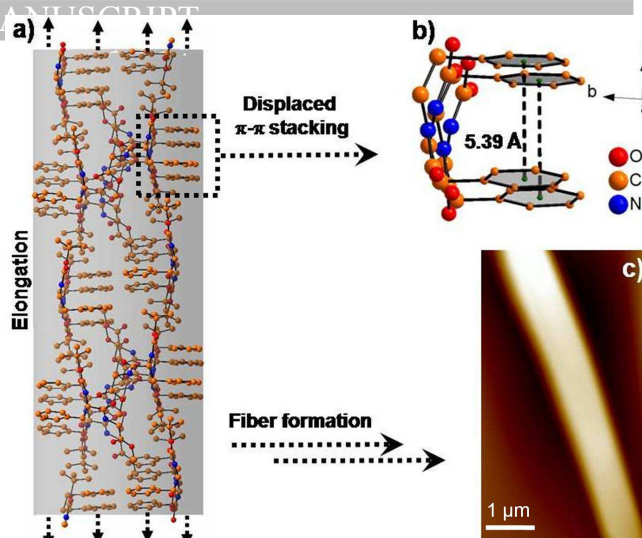


**Figure 10.** Solid state structure of (a) Boc-Phe-Gly-methyl ester "**1**" arranged in a columnar fashion (b) Displaced  $\pi$ - $\pi$  stacking (non bonded hydrogen's are omitted for the sake of clarity), (c) AFM micrograph of solution state self-assembly of **1**.

with a strong C-H... $\pi$  interactions between the hydrogen from tert-butyl group and phenylalanine aromatic ring along with other non covalent interactions. The elongation of crystal lattice directly correlates with AFM microscopic data where we have seen the straight fiber formation (Fig. 10c, 5C). Hydrogen bonding distances which are ranging from 2.05 Å-2.16 Å in solid state structure of **1** also help in columnar packing.

The challenging area of research in the ground of ordered supramolecular peptide assemblies by means of short peptides has been much focused in recent years.<sup>93, 94</sup> The construction of well-defined three dimensional hollow nanotubular assemblies by cyclic D and L-oligopeptides was advent of nanotechnology in past few decades and was contributed by Ghadiri and co-workers.<sup>95, 96</sup> It is known that synthetic tripeptide and terminally protected acyclic tripeptides self assembled into beeta-sheet type helical structures<sup>97</sup> or into polydispersed nanorods.<sup>98</sup> We also

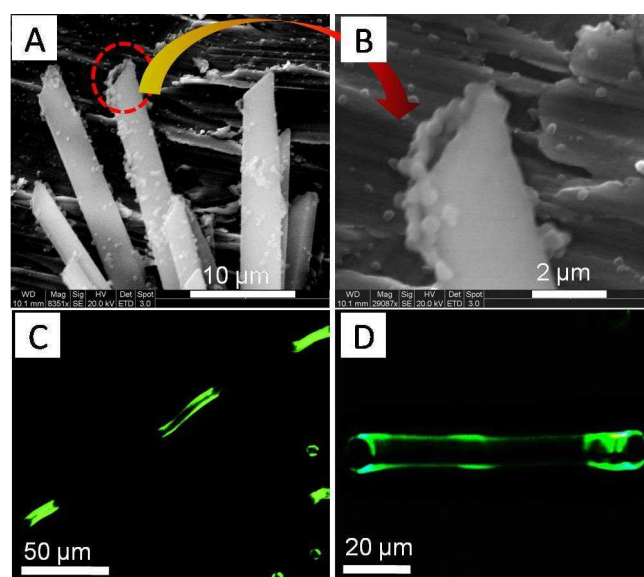


**Figure 11.** Depicts that (A, B) SEM images of conjugate **1** showing the hollowness of self assembled structures, (C, D) fluorescence optical microscopic images further confirming the cavity from the inner side.

observed that terminally protected elastomeric and amyloidogenic dipeptides sequences assembled into nanotubes or nanorods like structures. Our observations reveal that the D and L phenylalanine containing dipeptides produced well defined ordered structures compare to D and L proline one. We were able to confirm the nanostructures of phe containing dipeptide **1** is forming tubular structures, where the inside cavity is clearly visible under SEM (Fig. 11A, B). This observation was further supported by the

following experiments. The 40h pre incubated sample of **1** stained with fluorescein dye was, instantaneously analyzed<sup>90</sup> under fluorescence microscope using FITC filter in the dark field. These nanostructure appeared fluorescent green under the microscope and a dark lumen was observed at both the end of the tubular structures (Fig. 11C). The microscopic image of single tubular structures was further confirming these observations (Fig. 11D) where both the ends of the tubular structures are dark. Fluorescence detection is possible only when the dye is showing interaction with peptide molecules and since the structures are hollow from inside, therefore perhaps peptide cannot provide any active site at the void for dye interaction and therefore appearance of dark lumen under fluorescence optical microscope, especially at both the end of nanotubes.

### Conclusion

This report clearly demonstrates the formation of a supramolecular nanostructure in the solid state via hydrophobic interactions and hydrogen bonding from self-assembling elastomeric and amyloidogenic dipeptides constituents. The solid state assembly can directly be correlated with solution state self-assembling architectures. Further the phenylalanine containing dipeptides are making hollow tubular structures which give us the more insight of such sophisticated structure of nuclear pore complex and its tunneling mechanism. The selective permeability of NPC for different essential biomolecules and minerals and the transportation mechanism of nuclear membrane can easily be explained by these observations obtained by such solution phase self assembly of FG dipeptide. Such supramolecular nanotubular architectures of these dipeptides can show potential applications in the field of biomedical and nanotechnology. We have shown the difference between the self assemblies of the very simple dipeptide sequences and which perhaps is important for the design and construction of new, bioinspired nano-materials in the future. This report also indicates that not only cyclic peptides but also shortest acyclic peptides with suitable amino acid side chain that can form H-bonds with the main chain or side chain H-bonding group(s) may be used to construct nanochannels and nanotunnels.

### Experimental section

**General-** Dichloromethane, N, N-dimethylformamide, methanol and triethylamine were distilled following standard procedures prior to use. N, N'-dicyclohexylcarbodiimide, N-hydroxybenzotriazole, L-amino acids, glycine and N-hydroxysuccinimide were purchased from Spectrochem, Mumbai, India, and used without further purification. <sup>1</sup>H and <sup>13</sup>C NMR spectra were recorded on JEOL-JNM LAMBDA 400 model operating at 400 and 100 MHz, respectively. HRMS mass spectra were recorded at IIT Kanpur, India, on Waters, Q-Tof Premier Micromass HAB 213 mass spectrometer using capillary voltage 2.6-3.2 kV.

**Peptide synthesis** - All N-Boc-protected and de-protected peptide conjugates were synthesized by simple solution phase fragment condensation methodologies using <sup>t</sup>Boc chemistry and in the presence of HOBt. All the compounds were characterized well and satisfactory analytical spectroscopic results were also obtained for all the samples.

**Atomic Force Microscopy (AFM)** - Neat and co-incubated sample (at 37 °C for 0-5 days in methanol/water) solution of all the peptide conjugates were imaged with an atomic force microscope. The samples were placed on freshly cleaved muscovite mica surfaces and the sample-coated substrates were dried at dust free space under 60W lamp for 12h followed by high vacuum drying and subsequently examined under atomic force microscope (AFM). (INNOVA, ICON Analytical Equipment, Bruker, Sophisticated Instrument Center-Dr. Harisingh Gour Central University, Sagar-M.P.) operating under the Acoustic AC mode (AAC or Tapping mode), with the aid of a cantilever (NSC 12(c) from MikroMasch, Silicon Nitride Tip) by NanoDrive™ version 8 software. The force constant was 0.6 N/m, while the resonant frequency was 94-136 kHz. The images were taken in air at room temperature, with the scan speed of 1.5-2.2 lines/sec. The data analysis was done using of Nanoscope Analysis Software.

**Scanning Electron Microscopy (SEM)** - A solution of 20 μL aliquot of the fresh and aged samples of peptides were dried at room temperature on a copper stubs and coated with gold. Scanning electron microscopy images were made using a FEI QUANTA 200 microscope equipped with a tungsten filament gun operating at WD 10.6 mm and 20 kV. Concentration of peptide sample was 1 mM.

**Optical Microscopy-** Peptide self-assembled structures were examined under a fluorescent optical microscope (Leica DM2500M), in a dark field in addition to bright field under 63x. 1-3 mM of the peptide solution was incubated for 0-5 days in 50% methanol/water. 20 μL of this solution was spread on a glass slide and allowed to dry under petri dish in dust-free place at room temperature followed by imaging under optical microscope. For Fluorescein dye staining experiments, 2 days aged peptide samples were stained by these dye and 10μL of stained peptide samples were mounted on glass slides and allowed to dry under Petri dish in dust-free place. The dried samples were rinsed with distilled water 3×5s each for removal of excess and unbound dye. The excess water was dried and the samples were analyzed under polarized microscope.

**NMR titration experiments.** NMR titration experiments were carried out on JEOL-JNM LAMBDA 500 model spectrometer. 1D spectrum was recorded at a peptide concentration of 10 mg/400μL CDCl<sub>3</sub>, at 298 K. Description of exposed NH groups and other protons were achieved by titrating a CDCl<sub>3</sub> solution with low concentrations of CH<sub>3</sub>OH.

**Fourier Transform Infrared Spectroscopy:** Infrared spectra of peptide samples were recorded using a Bruker Vertex 70 Fourier transform infrared spectroscopy (FTIR) spectrometer with a resolution 4 cm<sup>-1</sup>, scan speed 2.5 kHz, and 128 scans co-addition, in the KBr pellet form. The obtained spectra were

smoothed by using the Savitsky-Golay algorithm to eliminate the noise. Peptide solutions were incubated at 37 °C followed lyophilization.

**Crystal structure refinement details for *tert*-Boc-L-Phe-Gly-OMe(1):** The compound was crystallized by the slow evaporation method. Data was collected on a Bruker SMART CCD4 X-ray diffraction instrument. The crystal was solved by direct methods and refined by using full-matrix least-squares on  $F^2$  (SHELX97). Crystal data for compound-1:  $C_{17}H_{24}N_2O_5$ ;  $M = 336.4$ , orthorhombic, space group P21 21 21 (No. 19),  $a = 10.62 \text{ \AA}$ ;  $b = 16.68 \text{ \AA}$ ;  $c = 20.68 \text{ \AA}$ ,  $V = 3667.26(4) \text{ \AA}^3$ ,  $Z = 8$ ,  $d = 1.22 \text{ g/cm}^{-3}$ ,  $T = 293(2) \text{ K}$ ,  $\mu(M_o-K) = 0.090 \text{ mm}^{-1}$ , 24535 reflections collected, 5025 independent reflection [ $R(int) = 0.0724$ ], final  $R1 = 0.093$ ,  $wR2 = 0.013$ (all data) [ $I > 2\sigma(I)$ ],  $R1 = 0.054$ ,  $wR2 = 0.0107$  (obs data). The structure was expanded using Fourier techniques. All other non-hydrogen atoms were refined anisotropically. Hydrogen atoms are placed at geometrically idealized positions. The final cycle of full-matrix least-squares refinement using SHELXL97 converged with unweighted and weighted agreement factors,  $R1 = 0.093$ ,  $wR2 = 0.013$ (all data), respectively, and goodness of fit,  $S = 1.049$ . The maximum and minimum peaks on the final difference Fourier map corresponded to 0.41 and  $-0.28 \text{ e \AA}^{-3}$ . CCDC contains the supplementary crystallographic data for this paper with a deposition number of **CCDC 670517**. Copies of this information can be obtained free of charge on application to CCDC, 12 Union Road, Cambridge CB2 1EZ, UK. [Fax: +44-1223/336-033; E-mail: deposit@ccdc.cam.ac or www.ccdc.cam.ac.uk.

**Crystal structure refinement details for *tert*-Boc-D-Phe-Gly-OMe(5):** The compound was crystallized by the slow evaporation method. Data was collected on a Bruker SMART CCD4 X-ray diffraction instrument. The crystal was solved by direct methods and refined by using full-matrix least-squares on  $F^2$  (SHELX97). Crystal data for compound-5:  $C_{17}H_{24}N_2O_5$ ;  $M = 336.4$ , orthorhombic, space group P21 21 21 (No. 19),  $a = 10.612 \text{ \AA}$ ;  $b = 16.67 \text{ \AA}$ ;  $c = 20.66 \text{ \AA}$ ,  $V = 3656.22(4) \text{ \AA}^3$ ,  $Z = 8$ ,  $d = 1.22 \text{ g/cm}^{-3}$ ,  $T = 293(2) \text{ K}$ ,  $\mu(M_o-K) = 0.090 \text{ mm}^{-1}$ , 9225 reflections collected, 5119 independent reflection [ $R(int) = 0.0724$ ], final  $R1 = 0.0675$ ,  $wR2 = 0.1909$ (all data) [ $I > 2\sigma(I)$ ]. The structure was expanded using Fourier techniques. All other non-hydrogen atoms were refined anisotropically. Hydrogen atoms are placed at geometrically idealized positions. The final cycle of full-matrix least-squares refinement using SHELXL97 converged with unweighted and weighted agreement factors,  $R1 = 0.0675$ ,  $wR2 = 0.1909$ (all data), respectively, and goodness of fit,  $S = 1.089$ . The maximum and minimum peaks on the final difference Fourier map corresponded to 0.41 and  $-0.28 \text{ e \AA}^{-3}$ . CCDC contains the supplementary crystallographic data for this paper with a deposition number of **CCDC 1440346**. Copies of this information can be obtained free of charge on application to CCDC, 12 Union Road, Cambridge CB2 1EZ, UK. [Fax: +44-1223/336-033; E-mail: deposit@ccdc.cam.ac or www.ccdc.cam.ac.uk

**Crystal structure refinement details for *tert*-Boc-Pro-Gly-OMethyl ester (2):** The compound was crystallized by the slow evaporation method. Data was collected on a Bruker SMART

CCD4 X-ray diffraction instrument. The crystal was solved by direct methods and refined by using full-matrix least-squares on  $F^2$  (SHELX97). Crystal data for compound-3:  $C_{13}H_{22}N_2O_5$ ;  $M = 286.32$ , orthorhombic, space group P21 21 21 (no. 19),  $a = 4.57 \text{ \AA}$ ;  $b = 14.48 \text{ \AA}$ ;  $c = 15.65 \text{ \AA}$ ,  $V = 1489.33(3) \text{ \AA}^3$ ,  $Z = 4$ ,  $d = 1.28 \text{ g/cm}^{-3}$ ,  $T = 293(2) \text{ K}$ ,  $\mu(M_o-K) = 0.098 \text{ mm}^{-1}$ , 10036 reflections collected, 2134 independent reflection [ $R(int) = 0.0664$ ], final  $R1 = 0.078$ ,  $wR2 = 0.126$ (all data) [ $I > 2\sigma(I)$ ],  $R1 = 0.057$ ,  $wR2 = 0.108$  (obs data). The structure was expanded using Fourier techniques. All other non-hydrogen atoms were refined anisotropically. Hydrogen atoms are placed at geometrically idealized positions. The final cycle of full-matrix least-squares refinement using SHELXL97 converged with unweighted and weighted agreement factors,  $R = 0.078$  and  $wR = 0.126$  (all data), respectively, and goodness of fit,  $S = 1.116$ . The maximum and minimum peaks on the final difference Fourier map corresponded to 0.387 and  $-0.269 \text{ e \AA}^{-3}$ . CCDC contains the supplementary crystallographic data for this paper with a deposition number of **CCDC 670518**. Copies of this information can be obtained free of charge on application to CCDC, 12 Union Road, Cambridge CB2 1EZ, UK. [Fax: +44-1223/336-033; E-mail: deposit@ccdc.cam.ac or www.ccdc.cam.ac.uk.

## Acknowledgements

VK thanks NFOBC-UGC-India for pre-doctoral research fellowship. KVK and SK thank IIT-Kanpur India for SRF. Authors thank Sophisticated Instrument Centre (SIC)- Dr. Harisingh Gour Central University Sagar-India for AFM and SEM facility. Our acknowledgment is incomplete without thanking Prof. Sandeep Verma, IIT Kanpur for his constant encouragements, invaluable support and for providing the research facility. This work is supported by UGC-BSR start-up scheme from University Grant Commission (UGC), India and Extramural Research Division, project no. 02(0238)/15/EMR-II from Council of Scientific and Industrial Research (CSIR) India to KBJ.

## Notes and references

1. Frederick, K. K.; Marlow, M. S.; Valentine K. G.; Wand, A. J. *Nature*, **2007**, *448*, 325-329.
2. Levy, Y.; Onuchic, J. N. *Annu Rev Biophys Biomol Struct.*, **2006**, *35*, 389-415.
3. Liao, J. J. L. *J. Med. Chem.*, **2007**, *50*(3), 409-424.
4. Bossi, A.; Bonini, F.; Turner, A. P. F.; Piletsky, S.A. *Biosen. Bioel.*, **2007**, *22*(6), 1131-1137.
5. Lyubchenko, Y. L.; Sherman, S. L.; Shlyakhtenko, S.; Uversky, V. N. *J. Cell Biochem.* **2006**, *99*(1), 52-70.
6. Mittag, T.; Kay, L. E.; Kay, J. D. F. *J. Mol. Recog.* **2009**, *23*(2), 105-116.
7. Hanessian, S.; Vinci, V.; Fettes, K.; Maris, T.; Viet, M. T. P. *J. Org. Chem.* **2008**, *73*, 1181-1191.
8. Nautiyal, S.; Woolfson, D. N.; King, D. S.; Alber, T. *Biochemistry*, **1995**, *34*, 11645-11651.
9. Ghadiri, R.; Soares, C.; Choi, C. *J. Am. Chem. Soc.*, **1992**, *114*, 825-831.
10. Hill, D. J.; Mio, M. J.; Prince, R. B.; Hughes, T. S.; Moore, J. S. *Chem. Rev.* **2001**, *101*, 3893-4012.
11. Sanford, A. R.; Gong, B. *Curr. Org. Chem.*, **2003**, *7*, 1649-1659.
12. Mashaghi, A.; Wijk, R. J. V.; Tans, S. J. *Structure*, **2014**, *22*, 1227-1237.

13. Operandi, M.; Uversky, V. N.; Kabanov, A. V.; Lyubchenko, Y. L. *J. Proteome Res.*, **2006**, *5*(10), 2505-2522.
14. Ray, S.; Drew, M. G. B.; Das, A. K.; Haldar, D.; Banerjee, A. *Tetrahedron Lett.*, **2006**, *47*, 2771-2774.
15. Buehler, J.; Yung, Y. C. *Nature Mat.*, **2009**, *8*, 175-188.
16. Monsellier, E.; Chiti, F. *EMBO reports*, **2007**, *8*(8), 737-742.
17. Tatham, A. S.; Shewry, P. R. *Trends Biochem. Sci.* **2000**, *25*(11), 567-571.
18. Cheng, S.; Cetinkaya, M.; Grater, F. *Biophys. J.*, **2010**, *99*, 3863-3869.
19. Li, H. B. *Adv. Func. Mat.*, **2008**, *18*, 2643-2657.
20. Cao, Y.; Li, H. *Nature Nanotech.*, **2008**, *3*, 512-516.
21. Lv, S.; Dudek, D. M.; Cao, Y.; Balamurali, M. M.; Gosline, J.; Li, H. *Nature*, **2010**, *465*, 69-73.
22. D'Angelo, M. A.; Hetzer, M. W. *Trends Cell Biol.* **2008**, *18*(10), 456-466.
23. Hoelz, A.; Debler, E. W.; Blobel, G. *Annu. Rev. Biochem.*, **2011**, *80*, 613-643.
24. Alber, F.; Dokudovskaya, S.; Veenhoff, L.; Zhang, W.; Kipper, J.; Devos, D.; Suprpto, A.; Karni-Schmidt, O.; Williams, R.; Chait, B. T.; Sali, A.; Rout, M. P. *Nature*, **2007**, *450*, 695-701.
25. Fahrenkrog, B.; Aeby, U. *Nat. Rev. Mol. Cell Biol.*, **2003**, *4*, 757-766.
26. Krull, S.; Thyberg, J.; Björkroth, B.; Rackwitz, H. R.; Cordes, V. C. *Mol. Biol. Cell*, **2004**, *15*(9), 4261-4277.
27. Tintar, D.; Samouillan, V.; Dandurand, J.; Lacabanne, C.; Pepe, A.; Bochicchio, B.; Tamburro, A. M. *Biopolymers*, **2009**, *91*(11), 943-952.
28. Foster, J. A.; Bruenger, E.; Grap, W. R.; Sandbergs, L. B. *The J. Biol. Chem.*, **1973**, *248*(8), 2876-2879.
29. Brown, C. P. *J. Mater. Res.*, **2015**, *30*(1), 108-120.
30. Vollrath, F.; Porter, D. *Soft Matter*, **2006**, *2*, 377-385.
31. Koebly, S. R.; Thorpe, D.; Pang, P.; Chrisochoides, P.; Greving, I.; Vollrath, F.; Schniepp, H. C. *Biomacromolecules*, **2015**, *16*(9), 2796-2804.
32. Chaw, R. C.; Correa-Garhwal, S. M.; Clarke, T. H.; Ayoub, N. A.; Hayashi, C. Y. *J. Proteome Res.* **2015**, *14*, 4223-4231.
33. Tokareva, O.; Michalczechen-Lacerda, V. A.; Rech, E. L.; Kaplan, D. L. *Microb Biotechnol.* **2013**, *6*(6), 651-663.
34. Tjin, M. S.; Low, P.; Fong, E. *Polymer Journal*, **2014**, *46*, 444-451.
35. Su, R. S.; Kim, Y.; Liu, J. C. *Acta. Biomater.*, **2014**, *10*(4), 1601-1611.
36. Elvin, C. M.; Carr, A. G.; Huson, M. G.; Maxwell, J. M.; Pearson, R. D.; Vuocolo, T.; Liyou, N. E.; Wong, D. C. C.; Merritt, D. J.; Dixon, N. E. *Nature*, **2005**, *437*, 999-1002.
37. Charati, M. B.; Ifkovits, J. L.; Burdick, J. A.; Linhardt, J. G.; Kiick, K. L. *Soft Matter*, **2009**, *5*, 3412-3416.
38. Denning, D. P.; Patel, S. S.; Uversky, V.; Fink, A. L.; Rexach, M. *PNAS*, **2003**, *100*(5), 2450-2455.
39. Savage, K. N.; Gosline, J. M. *J. Exp. Biol.*, **2008**, *211*, 1937-1947.
40. Rauscher, S.; Baud, S.; Miao, M.; Keeley, F. W.; Pome's, R. *Structure*, **2006**, *14*, 1667-1676.
41. Gosline, J. M.; Guerette, P. A.; Ortlepp, C. S.; Savage, K. N. *J. Exp. Biol.*, **1999**, *202*, 3295-3303.
42. Liu, Y.; Sponner, A.; Porter, D.; Vollrath, F. *Biomacromolecules*, **2008**, *9*(1), 116-121.
43. Allen, N. P. C.; Patel, S. S.; Huang, L.; Chalkley, R. J.; Burlingame, A.; Lutzmann, M.; Hurt, E. C.; Rexach, M. *Mol. Cell. Prot.*, **2002**, *1*, 930-946.
44. Doello, K. *J. Young Invest.*, **2013**, *25*(6), 87-95.
45. Gamin, R.; Han, W.; Stone, J. E.; Schulten, K. *PLOS Comput. Biol.*, **2014**, *24*(3), 1-14.
46. Alber, F.; Dokudovskaya, S.; Veenhoff, L. M.; Zhang, W.; Kipper, J.; Devos, D.; Suprpto, A.; Schmidt, O. K.; Williams, R.; Chait, B. T.; Sali, A.; Rout, M. P. *Nature*, **2007**, *450*(29), 695-701.
47. Denning, D. P.; Patel, S. S.; Uversky, V.; Fink, A. L.; Rexach, M. *Proc. Natl Acad. Sci. USA*, **2003**, *100*, 2450-2455.
48. Strawn, L. A.; Shen, T.; Shulga, N.; Goldfarb, D. S.; Wentz, S. R. *Nature Cell Biol.*, **2004**, *6*, 197-206.
49. Isgro, T. A.; Schulten, K. *J. Mol. Biol.*, **2007**, *366*, 330-345.
50. Bayliss, R.; Littlewood, T.; Stewart, M. *Cell*, **2000**, *102*, 99-108.
51. Denning, D. P.; Rexach, M. F. *Mol. Cell. Proteomics*, **2007**, *6*, 272-282.
52. Terry, L. J.; Wentz, S. R. *Eukaryot. Cell*, **2009**, *8*, 1814-1827.
53. Williams, A. D.; Portelius, E.; Khetarpal, I.; Guo, J.; Cook, K. D.; Xu, Y.; Wetzal, R. *J. Mol. Biol.*, **2004**, *335*(3), 833-842.
54. Xiao, S.; Stacklies, W.; Cetinkaya, M.; Markert, B.; Grater, F. *Biophys. J.*, **2009**, *96*, 3997-4005.
55. Vollrath, F.; Knight, D. P. *Nature*, **2001**, *401*, 541-548.
56. Gatesy, J.; Hayashi, C.; Motriuk, D.; Woods, J.; Lewis, R. *Science*, **2001**, *291*, 2603-2605.
57. Grubb, D. T.; Jelinski, L. W. *Macromolecules*, **1997**, *30*, 2860-2867.
58. Fedic, R.; Urovec, M. Z.; Sehnal, F. *J. Biol. Chem.*, **2003**, *278*, 35255-35264.
59. Denny, M. *J. Exp. Biol.*, **1976**, *65*, 483-506.
60. Rudall, K. M.; Kenchington, W. *Annu. Rev. Entomol.*, **1971**, *16*, 73-96.
61. Brooks, A. E.; Sticker, S. M.; Joshi, S. B.; Kamerzell, T. J.; Middaugh, C. R.; Lewis, R. V. *Biomacromolecules*, **2008**, *9*, 1506-1510.
62. Craig, C. L. *Biol. J. Linn. Soc.*, **1987**, *30*, 135-162.
63. Brown, C. P.; Rosei, F.; Traversa, E.; Licoccia, S. *Nanoscale*, **2011**, *3*, 870-876.
64. Brown, P. C.; Harnagea, C.; Gill, H. S.; Price, A. J.; Traversa, E.; Licoccia, S.; Rosei, F. *J. Am. Chem. Soc.*, **2012**, *6*(3), 1961-1969.
65. Chiba, T.; Hagihara, Y.; Higurashi, T.; Hasegawa, K.; Naiki, H.; Goto, Y. *J. Biol. Chem.*, **2003**, *278*, 47016-47024.
66. Moriarty, D. F.; Raleigh, D. P. *Biochemistry*, **1999**, *38*(6), 1811-1818.
67. Abedini, A.; Raleigh, D. P.; *J. Mol. Biol.*, **2006**, *355*(2), 274-281.
68. Myers, S. L.; Jones, S.; Jahn, T. R.; Morten, I. J.; Tennent, G. A.; Hewitt, E. W.; Radford, S. E. *Biochemistry*, **2006**, *45*(7), 2311-2321.
69. Mishra, N. K.; Kumar, V.; Joshi, K. B. *Nanoscale*, **2015**, *7*, 20238-20248.
70. Mishra, N. K.; Kumar, V.; Joshi, K. B. *RSC Adv.*, **2015**, *5*, 64387-64394.
71. Mishra, N. K.; Joshi, K. B.; Verma, S. *J. Colloid Interface Sci.*, **2015**, *455*, 145-153.
72. Joshi, K. B.; Singh, P. *Tetra. Lett.*, **2014**, *55*(25), 3534-3537.
73. Valéry, C.; Artzner, F.; Paternostre, M. *Soft Matter*, **2011**, *7*, 9583-9594.
74. Lakshmanan, A.; Cheong, D. W.; Accardo, A.; Di Fabrizio, E.; Riekel, C.; Hauser, C. A. E. *Biophys. Comp. Biol.*, **2013**, *110*(2), 519-524.
75. Davies, R. P. W.; Aggeli, A.; Boden, N.; McLeish, T. C.B.; Nyrkova, I. A.; Semenov, A. N. *Adv. Chem. Eng.*, **2009**, *25*, 11-43.
76. Gatesy, J.; Hayashi, C.; Motriuk, D.; Woods, J.; Lewis, R. *Science*, **2001**, *291*(5513), 2603-2605.
77. Porat, Y.; Abramowitz, A.; Gazit, E. *Chem. Biol. Drug. Des.*, **2006**, *67*, 27-37.
78. Carugo, O.; Bordo, D. *Acta. Crystallogr. D. Biol. Crystallogr.*, **1999**, *55*(2), 479-483.
79. Spek, A. L. *Acta Cryst.* **2009**, *65*(2), 148-155.
80. Lu, Y.; Wang, R.; Yang, C. Y.; Wang, S. *J. Chem. Inf. Model*, **2007**, *47*(2), 668-675.
81. Ross, G. A.; Morris, G. M.; Biggin, P. C. *PLoS ONE*, **2012**, *7*(3), 1-13.
82. Kim, Y.; Kim, T.; Lee, M. *Polym. Chem.*, **2013**, *4*, 1300-1308.
83. Furuya, T.; Kiyota, T.; Lee, S.; Inoue, T.; Sugihara, G.; Logvinova, A.; Goldsmith, P.; Ellerby, H. M. *Biophys. J.*, **2003**, *84*(3), 1950-1959.
84. Reches, M.; Gazit, E. *Phys. Biol.* **2006**, *3*, 10-19.
85. Maji, K.; Sarkar, R.; Bera, S.; Haldar, D. *Chem. Commun.*, **2014**, *50*, 12749-12752.
86. Matsumura, S.; Uemura, S.; Mihara, H. *Chem. Eur. J.*, **2004**, *10*, 2789-2794.
87. Matsumura, S.; Uemura, S.; Mihara, H. *Mol. BioSyst.*, **2005**, *1*, 146-148.
88. Maity, S.; Jana, P.; Maity, S. K.; Haldar, D. *Langmuir*, **2011**, *27*, 3835-3841.
89. Woolfson, D. N.; Ryadnov, M. G. *Current Opin. Chem. Biol.* **2006**, *10*(6), 559-567.
90. Joshi, K. B.; Verma, S. *Angew. Chem. Int. Ed.*, **2008**, *47*, 2860-2863.
91. Berl, V.; Huc, I.; Khoury, R. G.; Krische, M. J.; Lehn, J. M. *Nature*, **2000**, *407*, 720-723.
92. Haldar, D.; Banerjee, A.; Drew, M.G. B.; Das, A. K.; Banerjee, A. *Chem. Commun.*, **2003**, 1406-1407.
93. Nautiyal, S.; Woolfson, D. N.; King, D. S.; Alber, T. *Biochemistry*, **1995**, *34*, 11645-11651.
94. Hill, D. J.; Mio, M. J.; Prince, R. B.; Hughes, T. S.; Moore, J. S. *Chem. Rev.*, **2001**, *101*, 3893-4012.
95. Ghadiri, M. R.; Granja, J. R.; Milligan, R. A.; Mckee, D. E.; Khazanovich, N. *Nature*, **1993**, *366*, 324-327.
96. Aizman, K. R.; Svensson, G.; Uden, A. *J. Am. Chem. Soc.*, **2004**, *126*, 3372-3373.
97. Das, A. K.; Haldar, D.; Hegde, R. P.; Shamala, N.; Banerjee, A. *Chem. Commun.*, **2005**, 1836-1838.
98. Bera, S.; Jana, P. I.; Maity, S. K.; Haldar, D. *Cryst. Growth Des.*, **2014**, *14*(3), 1032-1038.
99. Reches, M.; Gazit, E. *Phys. Biol.* **2006**, *3*: S10-S19.
100. Tamburro A.M., Pepe A, Bochicchio B., Quaglino D, Ronchetti I.P. *J. Biol. Chem.* **2005**, *280*, 2682-2690.
101. Aggeli A, Nyrkova IA, Bell M, Harding R, Carrick L, McLeish TCB, Semenov A.N, Boden N. *Proc. Natl. Acad. Sci. U.S.A.* **2001**, *98*, 11857-11862.
102. Joshi, K.B.; Verma, S. *J. Pep. Sci.* **2008**, *14*, 118.